The Protein Journal (2020) 39:501–508
https://doi.org/10.1007/s10930-020-09920-1

Aldehyde Production as a Calibrant of Ultrasonic Power Delivery During Protein Misfolding Cyclic Amplification

Simon C. Drew[1,2]

Accepted: 28 September 2020 / Published online: 3 October 2020

Abstract
The protein misfolding cyclic amplification (PMCA) technique employs repeated cycles of incubation and sonication to amplify minute amounts of misfolded protein conformers. Spontaneous (de novo) prion formation and ultrasonic power level represent two potentially interrelated sources of variation that frustrate attempts to replicate results from different laboratories. We previously established that water splitting during PMCA provides a radical-rich environment leading to oxidative damage to substrate molecules as well as the polypropylene PCR tubes used for sample containment. Here it is shown that the cross-linking agent formaldehyde is generated from buffer ions that are attacked by hydroxyl radicals. In addition, free radical damage to protein, nucleic acid, lipid, and detergent molecules produces a substantial concentration of aldehydes (hundreds of micromolar). The measurement of aldehydes using the Hantzsch reaction provides a reliable and inexpensive method for measuring the power delivered to individual PMCA samples, and for calibrating the power output characteristics of an individual sonicator. The proposed method may also be used to better account for inter-assay and inter-laboratory variation in prion replication and de novo prion generation, the latter of which may correlate with aldehyde-induced cross-linking of substrate molecules.

Keywords Protein misfolding cyclic amplification · Prion · Ultrasound · Aldehyde · Formaldehyde

1 Introduction

Protein misfolding cyclic amplification (PMCA) was developed with the objective of detecting very small amounts of protease-resistant prion protein (PrP^{Sc}), a surrogate marker of transmissible neurodegenerative diseases such as Creutzfeldt Jakob Disease (CJD) and bovine spongiform encephalopathy. The process of PMCA involves seeding natively-folded PrP^{C} (from whole brain, cell culture, or recombinant expression) with a minute quantity of infectious PrP^{Sc}, followed by repeated cycles of incubation and sonication [1]. A templating interaction of PrP^{C} with PrP^{Sc} causes seeded protein misfolding and elongation of the PrP^{res} polymer. The 20 kHz sonication step in PMCA was introduced to fragment the growing polymer, exposing more PrP^{Sc} to the substrate and producing an exponential increase in prion replication [2]. PMCA is therefore viewed as a means to accelerate the conversion process that occurs in vivo, enabling the presence of PrP^{Sc} in the original titre to be inferred upon immunodetection of the amplified PrP^{res}. Contamination of otherwise non-infectious samples, or the de novo (spontaneous) generation of infectious PrP from non-infectious substrate, can produce false positives when using PMCA to screen for prion disease. De novo prion formation [3–6], as opposed to propagation/amplification of an existing prion [7, 8], requires RNA and lipid as essential cofactors, and has not been observed in vitro in the absence of sonication. The molecular mechanism underlying this phenomenon remains unknown, but we have proposed that it involves a confluence of structural (membrane-mimetic) and chemical (free radical) conditions present during the sonication step of PMCA [9]. We previously demonstrated that these radicals and reactive oxygen species (ROS) created

Electronic supplementary material The online version of this article (https://doi.org/10.1007/s10930-020-09920-1) contains supplementary material, which is available to authorized users.

✉ Simon C. Drew
sdrew@unimelb.edu.au

[1] Department of Medicine (Royal Melbourne Hospital), The University of Melbourne, Victoria 3010, Australia

[2] Institute of Biochemistry and Biophysics, Polish Academy of Sciences, Warsaw 02-106, Poland

during 20 kHz sonication lead to formation of PrP- and RNA-centred radicals, RNA oxidation, protease-resistant covalent PrP-RNA adducts [9]. In this study, we sought to quantify oxidative damage to these and other components of the PMCA substrate (including Tris, Triton X-100) by measuring their conversion to aldehydes by sonolytically-produced hydroxyl radicals. The results demonstrate that even bystander molecules undergo radical damage during the PMCA method, which can lead to a number of cross-linking interactions that may underpin the stochastic creation of synthetic PrP-containing molecules that possess infectivity to wild type mice (de novo prions). Notably, the formation of aldehydes offers a means to calibrate the power delivered to substrates by individual sonicators, which can improve the correlation of results between laboratories and may also correlate the frequency of de novo events with the delivered sonicator power and oxidative damage.

2 Materials and Methods

2.1 Reagents

Tris-buffered saline (TBS; 10 mM Tris, 150 mM NaCl, pH 7.5) was obtained from G-BioSciences. Bis–Tris (bis(2-hydroxyethyl)amino-tris(hydroxymethyl)methane), acetylacetone and 2-Oleoyl-1-palmitoyl-sn-glycero-3-phospho-rac-(1-glycerol) sodium salt (POPG), ammonium acetate and acetic acid were obtained from Sigma-Aldrich. Peroxide-free 10% w/v aqueous Triton X-100 (octylphenol ethylene oxide condensate) solution was obtained from Amresco. 5,5-dimethyl-1-pyrroline-*N*-oxide (DMPO) was obtained from Alexis Biochemicals and used without further purification. Bacterially-expressed α-folded recombinant murine $PrP_{23–231}$ was obtained from Prionatis. Mouse total RNA (whole brain) was purchased from Agilent Technologies. Nuclease-free water was from Qiagen. Thin-walled, RNAase-free 0.2 mL PCR tubes were obtained from Scientific Specialties Inc. Deionised water had a resistivity of 18 MΩ cm (Milli-Q®, Millipore).

2.2 Sample Preparation

Samples contained either buffer alone, Triton X-100 in buffer, complete PMCA substrate preparation used for creating de novo prions from recombinant PrP. The PMCA substrate preparation followed the original protocol used for de novo prion experiments [3, 4, 9] except for the use of total RNA from whole mouse brain in place of total RNA from mouse liver, and the preparation of SUVs by extrusion through a 50 nm polycarbonate membrane (Avanti Polar Lipids); final reagent concentrations: $[PrP_{23–231}] = 0.2$ μM, [RNA] = 0.03 mg/mL, [POPG] = 6 μM, [Triton X-100] = 4.3 mM (0.28% w/v), [Tris HCl] = 10 mM, [NaCl] = 150 mM, pH 7.5. All samples had 100 μL volume and were contained in sterile PCR tubes.

2.3 Sonication

Sample tubes were sealed around the lid using Parafilm (Bemis Company, USA) and placed in a plastic microcentrifuge tube adapter (part # 444) positioned above the microplate horn accessory (part # 431MPH) of a model S-4000 sonicator (Misonix, USA) (Fig. 1a). Four replicate sample tubes were positioned in the centre of the adapter tray with one empty sample position separating each tube (Fig. 1a). The horn reservoir was filled with 200 mL distilled water and the PCR tubes positioned ca. 1 mm above the surface of the horn (Fig. 1b). Sonication powers in the range 0–300 W were applied by adjusting the amplitude setting on the Misonix display to achieve the approximate power desired. To mimic the PMCA procedure, 48 cycles of 20 kHz sonication were applied for 30 s every 30 min (Fig. 1c), corresponding to one round of PMCA. The average power delivered over the entire 48 cycles was determined by dividing the total energy delivered (read from the Misonix display) by the sonication time (48×30 s = 1440 s). After the completion of the cyclic sonication, sample tubes were transferred to − 80 °C storage until further analysis.

2.4 Aldehyde Measurement

Two independent methods were used. The first employed a proprietary fluorescent formaldehyde detection kit (Invitrogen, EIACH2O) and the second used a colorimetric/fluorometric assay based on the established Hantzsch reaction (Fig. 1d) [10–12].

Using the proprietary formaldehyde detection kit, standard samples (0–200 μM) were freshly prepared in deionised water using the supplied 2 mM formaldehyde standard. Fifty microliters of each sample (in quadruplicate) or standard (in duplicate) was combined with 25 μL proprietary detection reagent in the wells of a black, half-volume, 96-well plate. The plate was incubated at 37 °C for 30 min, then fluorescence of each well was measured using a microplate reader (FLUOstar Optima; BMG Labtech) fitted with 450 nm excitation and 510 nm emission filters. Formaldehyde concentration of each sample was determined from the average fluorescence of the four replicate wells, with reference to a calibration curve generated from the average fluorescence of formaldehyde standards measured in duplicate wells. Each assay was repeated three times ($n = 3$).

For detection of aldehydes using the Hantzsch assay, the Hantzsch reagent was prepared by combining 1.54 g ammonium acetate, 28.6 μL glacial acetic acid and 20.5 μL acetylacetone with deionised water to a final volume

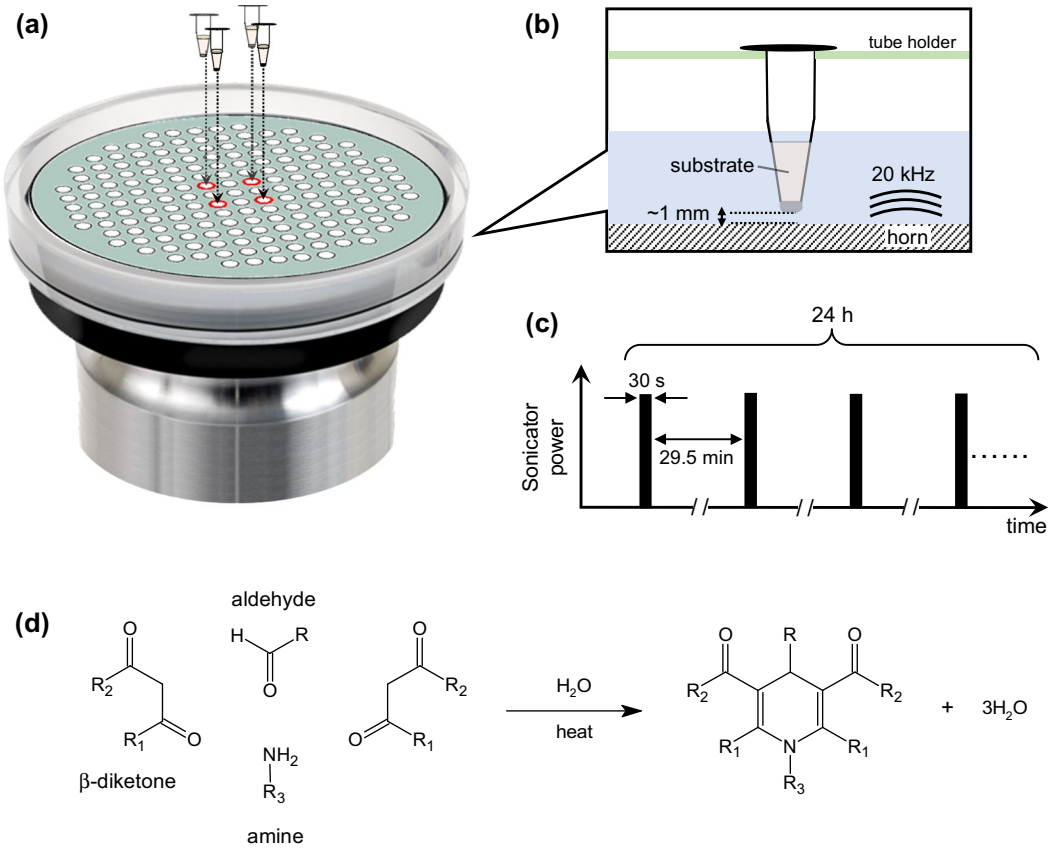

Fig. 1 **a** Experimental setup of the ultrasonic processor (Misonix, S-4000) used for protein misfolding cyclic amplification (PMCA), with polypropylene PCR tubes positioned in the centre of the Perspex tube holder (Misonix, #444). **b** Tubes containing 100 µL substrate were positioned approximately 1 mm above the surface of a microplate horn (Misonix, #431MPX, 15 cm diameter) filled with 200 mL deionised water, and **c** 48 cycles of 20 kHz sonication (30 s) and incubation (29.5 min) were applied (equivalent to one round of PMCA). **d** Hantzsch reaction between an aldehyde (RCHO), a β-diketone ($R_1CHOCH_2CHOR_2$), an amine (R_3NH_2), producing a coloured (A_{max} = 412 nm). To measure aldehydes produced during PMCA, acetylacetone (R_1=R_2=CH_3) and ammonium acetate (R_3=H) were used as the Hantzsch reagent

of 10 mL (final concentrations of 2 M ammonium acetate, 0.05 M acetic acid, 0.02 M acetylacetone). Ten microliters from each of the four replicate samples were combined in a 1.5 mL microcentrifuge tube, then 20 µL Hantzsch reagent was added. Forty microliters of formaldehyde standards (prepared using the same 2 mM standard supplied with the fluorescence detection kit) were also combined with 20 µL Hantzsch reagent. The tubes were incubated in 37 °C water bath for 40 min, then the absorbance at 412 nm was read using a SPECTROstar Nano UV–Vis spectrometer (BMG LABETCH) with a 50 µL disposable cuvette (UVette, Eppendorf). The aldehyde concentration in each sample was determined using a calibration curve generated from the formaldehyde standards. Interference from alkylamines in the sample (buffer molecules, protein, and nucleic acid) is low because of their relatively slow rate of reaction compared with excess ammonium ions [10].

2.5 Statistical Analyses

GraphPad Prism version 8.4.2 for Windows (GraphPad Software, San Diego, California USA, www.graphpad.com) was used for all statistical comparisons and segmental regression analysis. Residual analysis of some samples failed tests of normality required for parametric analysis of variance (ANOVA). Therefore, nonparametric two-way ANOVA was performed using an aligned rank transform followed by a full-factorial ANOVA of the transformed data, as described by Wobbrock et al. [13]. In contrast to parametric methods, the aligned rank transform does not permit cross-factor pairwise multiple comparisons; therefore, post hoc comparisons were made only within a single factor (no interaction). Values quoted in the text correspond to mean ± SEM unless stated otherwise.

3 Results

3.1 PMCA Produces Formaldehyde from Tris Buffer

Hydroxyl radicals have been reported to degrade a range of buffer ions containing hydroxymethyl or hydroxyethyl groups into formaldehyde [14]. We have previously demonstrated that hydroxyl and hydrogen radicals are produced during 20 kHz sonication [9]. Therefore, we began by applying 24 h of cyclic sonication (30 s) and incubation (29.5 min) to Tris-buffered saline (equivalent to one round of PMCA). As anticipated, formaldehyde was detected at the end of the round (Fig. 2a). Although the concentration of 33 ± 1 µM formaldehyde is low compared with the total Tris concentration (10 mM), it is 2–3 orders of magnitude higher than the concentration of PrP used for PMCA assays [1, 3].

The mechanism of formaldehyde formation from Tris remains unclear, however the primary amine group has been identified as a site of hydroxyl radical attack. To assess the role of the amine, TBS was substituted with bis–Tris buffered saline (BTBS; 10 mM bis–Tris, 150 mM NaCl, pH 7.5). Bis–Tris was previously reported to produce negligible formaldehyde in the presence of a Fenton system [14]; however, in the present case, sonication of bis–Tris generated 20 ± 1 µM formaldehyde (Fig. 2b), suggesting that the tertiary amine of bis–Tris is merely a less facile site of hydroxyl radical attack or that different free radical pathways are possible during 20 kHz sonication. Interestingly, the addition of the radical-trapping agent DMPO (100 mM) to TBS resulted in a higher yield of formaldehyde than sonication of TBS alone (Figure S1). This suggests that either a minor fraction of DMPO is itself degraded to a (form)aldehyde product or that DMPO intercepts a fraction of the hydroxyl radicals that would otherwise oxidise the TBS-derived formaldehyde to formic acid [15]. We do not concern ourselves further with such matters here, instead focussing on the empirical observation that the buffer used to create synthetic de novo prions from recombinant PrP [3, 4] is not an inert bystander during cyclic 20 kHz sonication.

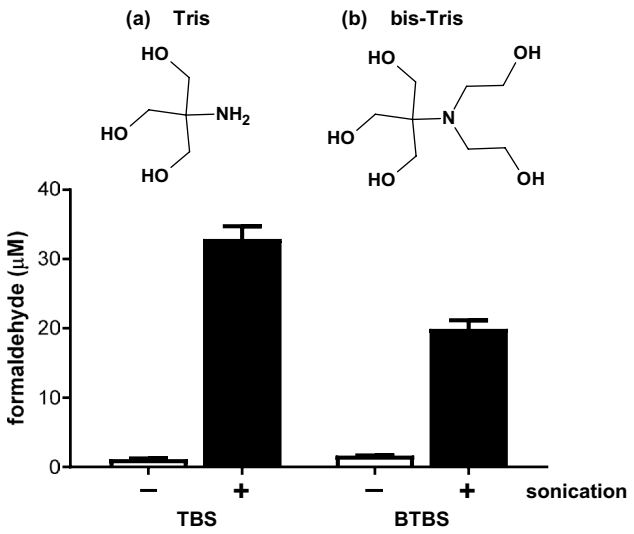

Fig. 2 Formaldehyde measured after 24 h incubation at 37 °C with (+) or without (−) cyclic sonication (30 s at 300 W every 30 min) of **a** Tris-buffered saline (TBS) and **b** bis–Tris-buffered saline (BTBS) ($n = 3$, mean ± SD). Using two-way non-parametric ANOVA, the main effects of *cyclic sonication* ($F_{1,8} = 26.31$, $p < 0.0009$) and *buffer type* ($F_{1,8} = 26.31$, $p < 0.0009$) are equally significant, and their interaction is also significant ($F_{1,8} = 26.05$, $p < 0.0009$)

3.2 Formaldehyde Production from Tris Buffer Correlates with Ultrasonic Power

We next assessed the formaldehyde production as a function of sonication power. Non-negligible formaldehyde levels were measured only when the average sonicator power exceeded a value of 160 ± 10 W/cm^2, above which the formaldehyde concentration increased monotonically (Fig. 3). This value is ascribed to the threshold for achieving transient cavitation, which is responsible for sonochemical effects [16]. Although many factors affect the threshold power (temperature, heat capacity of dissolved gases, solution viscosity, surface tension, vapour pressure, the geometry and thickness of sample tubes, and their positioning relative to the transducer), the measured transition point is comparable with powers typically required to achieve cavitation at 20 kHz [17], and with the minimum average power necessary for efficient amplification of PrP^{Sc} using the same ultrasonicator [18]. Comparison of segmental regression analyses yielded no difference between the Hantzsch assay (Fig. 3a) and the proprietary fluorometric assay (Fig. 3b). The relatively large variation in the measured formaldehyde concentration at 200 W suggests that operation close to cavitation threshold produces an outcome that is highly sensitive to the precise sample positioning. Figure S2 shows the same data together with the 95% confidence intervals, from which it is clear that PMCA experiments operating near the cavitation threshold can provide a major source of inter-assay variation.

3.3 Aldehyde Production from Substrate Molecules During PMCA

The Hantzsch reaction proceeds for all aldehydes (Fig. 1d), including those formed during the oxidative damage to substrate molecules used for de novo creation of synthetic prions (PrP, nucleic acid, detergent, lipid). Triton X-100 is a non-ionic surfactant that is incorporated into PMCA protocols to promote solubility of misfolded PrP [3, 19]. With the possible exception of buffer molecules, it is usually present at the highest concentration of any cofactor. It can also contain

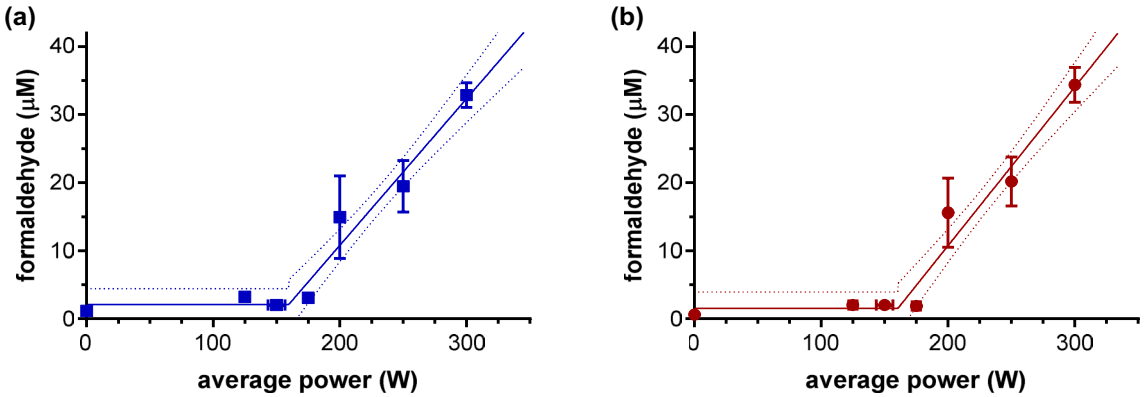

Fig. 3 Formaldehyde measured after 24 h of cyclic 20 kHz sonication (30 s at 250 W) and incubation (29.5 min) of TBS at 37 °C using different ultrasonic powers ($n=3$, mean ± SD). Results from **a** the Hantzsch assay are compared with those from **b** a proprietary formaldehyde detection kit. The solid and dashed lines show the segmental linear regression and the associated 95% confidence intervals; the cavitation threshold is (a) 160 ± 9 W and (b) 161 ± 9 W, above which formaldehyde is produced at (a) 0.22 ± 0.02 μM/W and (b) 0.23 ± 0.02 μM/W. Goodness of fit parameter: (a) $R^2=0.927$. (b) $R^2=0.933$

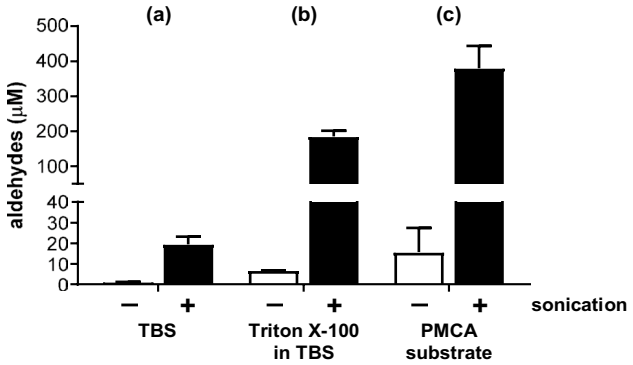

Fig. 4 Comparison of aldehyde concentration measured after 24 h incubation at 37 °C with (+) or without (−) cyclic sonication (30 s at 300 W every 30 min) of **a** TBS, **b** 0.28% w/v Triton X-100 in TBS, and **c** PMCA substrate (0.2 μM $PrP_{23–231}$, 0.03 mg/mL total RNA, 6 μM POPG, 0.28% w/v Triton X-100, TBS pH 7.5). Total aldehydes were measured as equivalents of formaldehyde using the Hantzsch reaction ($n=3$, mean ± SD). Using two-way nonparametric ANOVA, the main effects of *cyclic sonication* ($F_{1,12}=38.15$, $p<0.0001$) and *sample composition* ($F_{2,12}=51.16$, $p<0.0001$) are significant, and their interaction is also significant ($F_{2,12}=54.50$, $p<0.0001$). Within-effects analysis of *sample composition* (averaged over the levels of *sonication*): TBS vs Triton X-100, $p=0.0008$; TBS vs PMCA substrate, $p<0.0001$; Triton X-100 vs PMCA substrate, $p=0.0008$ (Tukey multiple comparison tests)

up to 2% impurities from carbonyl compounds such as carboxylic acids, ketones or aldehydes. Therefore, we determined the aldehyde content of our source of Triton X-100 at the concentration used for creating synthetic de novo prions (0.28% w/v [3, 4]) in TBS. Untreated Triton X-100 was found to contain a relatively modest concentration (6.7 ± 0.2 μM) of aldehydes (Fig. 4). Surfactant molecules are known to accumulate radially at the gas–liquid interface of cavitation bubbles [20], exposing Triton X-100 molecules to the highest concentration of free radicals. Consistent with a high degree of oxidative degradation, 185 ± 16 μM aldehydes were measured after 24 h cyclic 20 kHz sonication (30 s at 250 W) and incubation (29.5 min) of 0.28% w/v Triton X-100 (Fig. 4). The untreated PMCA substrate (PrP, RNA, POPG, Triton X-100 in TBS) contained 16 ± 12 μM aldehydes (Fig. 4), which increased to 380 ± 63 μM after 24 h cyclic sonication. This value is approximately twice that measured for Triton X-100 alone, suggesting that half of the aldehyde content arises from oxidative damage to PrP, RNA, and POPG.

4 Discussion

Ultrasonication exposes PrP and cofactor molecules to primary hydroxyl and hydrogen radicals, together with a range of secondary radicals and oxidants, at or near the surface of cavitation bubbles. The hydroxyl radical is a highly reactive oxidant that can undergo addition reactions (hydroxylation) with C=C and C=N bonds (such as those found in purines of nucleic acid) and abstract H atoms from C–H and N–H groups, yielding carbon- and nitrogen-centred radicals [21]. The complexity of the ensuing radical cascades increases in proportion to the number of reactants and their molecular weight, making it impossible to fully understand the advanced oxidation processes that occur [22–24]. However, it is clear that PMCA exposes PrP to more than the fragmenting and templating steps that are believed to underpin the process of PrP^{res}.

Here, we focus on aldehydes produced by cyclic sonication, which can be measured using the Hantzsch reaction. Hydroxyl radicals produce formaldehyde from many Good's [14] buffers, including Tris and HEPES, both of

which are used as PMCA conversion buffers [3, 19]. In the present case, approximately 5% of the total aldehydes produced during PMCA can be ascribed to formaldehyde derived from TBS alone (Fig. 4a), with formaldehyde concentration monotonically increasing as a function of sonicator power above the cavitation threshold (Fig. 3). Approximately half of the total aldehyde can be attributed to oxidation of Triton X-100 (Fig. 4b); hydroxyl radical addition to the hydrophobic octylphenol head group of Triton X-100 and abstraction of hydrogen atoms from the hydrophobic poly(ethylene oxide) chains have been reported [25], although precise oxidation products were not identified. The remaining proportion of aldehydes produced during PMCA results from oxidation of protein, nucleic acid, and lipid (Fig. 4c). Oxidation of protein side chains leads to formation of carbonyls (aldehydes and ketones) [26, 27]. Hydroxyl radicals can cleave the glycosyl bond of nucleic acid, creating an apurinic/apyrimidinic site whose resonance structures involve an open-chain aldehyde [28]. Similar to Triton X-100 [20], POPG will accumulate radially at the gas–liquid interface of cavitation bubbles, exposing the fatty acid chains to hydroxyl radicals [9] that can readily react with the double bond of the oleoyl chain to yield an aldehyde [29].

In some PMCA protocols, a higher concentration of 1% w/v Triton X-100 is used [19]. In such cases, aldehyde production from the detergent could exceed that produced from all other PMCA substrate molecules. Ethylenediaminetetraacetic acid (EDTA) is included in some protocols for creating synthetic de novo prions [5]. Here, hydroxyl radicals attack can EDTA, yielding nitrogen- and carbon-centred EDTA radicals that lead to formation of a number of products including formaldehyde and the aldehyde [(2-Oxoethyl) imino]diacetic acid [30].

Both aldehydes and ketones can undergo reversible nucleophilic addition reactions with amines (e.g. lysine ε-amino group, endo- and exocyclic amino groups of nucleobases [31–33]) to form imines [34] that can react with a nucleophile from a second molecule to yield a reversible covalent cross-link [35–38]. The nucleophilic addition reactions underpinning imine formation are favoured at a mildly acidic pH [34]. Oxidation of dissolved N_2 in aerated solutions forms nitric oxide and nitrogen dioxide radicals that react with hydroxyl radicals to produce nitrous (HNO_2) and nitric (HNO_3) acid, respectively [39, 40]. Lower pH can also be promoted by the formic acid produced from the oxidation of formaldehyde by hydroxyl radicals [15]. Because these reactions take place near the gas–liquid interface, where the transient hydroxyl radicals are most concentrated, this can reduce the local pH to a value that promotes imine formation and cross-linking even if the bulk pH remains relatively stable. The low pH at the interface may also promote PrP misfolding [41, 42] and prion formation [43].

Reactive oxygen and nitrogen species also lead to many other protein-nucleobase cross-links [44]. Peroxynitrite is formed by the reaction of nitric oxide (vide supra) with superoxide (derived from secondary reactions of hydroxyl radicals) that can diffuse away from cavitation bubbles into the bulk solution [40] and cause protein nitrosylation and RNA damage [45]. Formic acid produced by oxidation of formaldehyde [15] can also covalently modify protein side chains, particularly by O-formylation of serine [46].

4.1 Relevance to Creation of De Novo Synthetic Prions and Prion Diagnostics

Because the above phenomena are triggered by primary hydroxyl radicals, all are physiologically relevant. Although some of the formaldehyde generated during PMCA is derived from non-physiological molecules (e.g. Tris), the effects of this formaldehyde on other substrate molecules may be relevant to the spontaneous creation of de novo prions from non-infectious recPrP substrate [3]. Formaldehyde results from many physiological processes [47–49] and an imbalance of endogenous formaldehyde metabolism has been proposed as a trigger for age-related cognitive decline because of its ability to cause β-amyloid aggregation and tau hyperphosphorylation in vivo [50].

Because aldehydes are formed in response to free radicals at the surface of cavitation bubbles, the Hantzsch assay offers a means to correlate these sonochemical phenomena with de novo prion generation. Quaking-induced conversion (QuIC) methods, involving extended shaking of the substrate, have been used to induce the misfolding of recPrP into thioflavin-T-reactive amyloid in the presence of infectious seeds [51], but QuIC products do not possess infectivity [52]. By operating in a power range below the threshold for aldehyde production (i.e. below the cavitation threshold), mechanical fragmentation of the PrP aggregates could be achieved without the unique physicochemical phenomena that accompany cavitation. If de novo prion generation is eliminated under such conditions but does not prevent the amplification of pre-existing PrP^{Sc} seeds, then 'false positives' could be avoided when using PMCA as a diagnostic tool; moreover, this would provide support for the hypothesis that de novo generation of synthetic prions relies on free radical-mediated phenomena at the surface of membrane-mimetic cavitation bubbles [9].

4.2 Comparison with Other Methods for Measuring Ultrasonic Power

A calorimetric method can be used as a measure of acoustic power [53]. However, this requires the local

temperature change of the sample solution to be measured, which is impractical for PMCA, where the sample tubes usually contain very small volumes, many such tubes are sonicated in parallel, and ultrasound energy is transferred indirectly via a water bath. Another surrogate method of measuring ultrasonic power relies on the reaction of sonochemically liberated H_2O_2 with KI, which is oxidised to I_3^- and spectrophotometrically detected at 353 nm [53–55]. The KI can be added before or after sonication [55], although its inclusion during sonication is an undesirable modification of the usual PMCA substrate preparation. Addition of KI after sonication will measure any H_2O_2 remaining at the end of the PMCA round, but this may not correlate with the cumulative free radical damage to substrate molecules.

The calorimetric and KI oxidation methods have been used to map the ultrasonic power at specific positions across the base of a sonicating water bath [56], and this pre-calibration was used to infer the energy delivered to recPrP samples that were subsequently positioned at those same locations. These methods were shown to be excellent measures of sonochemical efficiency, and could be used to correlate ultrasonic power with formation of specific types of PrP amyloid [56]; however, the pre-calibration provides only an indirect prediction of the energy absorbed by an individual PMCA sample, which varies stochastically. In comparison, the present method permits a direct measurement of the relative power delivered to an individual sample by quantifying the sonochemical production of aldehydes.

5 Conclusions

The ultrasonic field experienced by an individual sample during PMCA can vary significantly between and within instruments. The total aldehyde content, measured using the Hantzsch assay with either colorimetric [10] or fluorometric [11, 12] readout, can be used as a surrogate marker of ultrasonic power delivered to an individual sample. This offers a simple way to assess the importance of free radical phenomena in the creation of de novo prions, and to better correlate results obtained by different diagnostic laboratories.

Funding This work was supported by a grant awarded by the Australian Creutzfeldt–Jakob Disease Support Group Network (CJDSGN) in memory of Silva Coelho, and a grant awarded by the CJDSGN in memory of Frank Burton, Bassil Gianniodis, Primo Monaci, Rhonda Sanders, Cesarina Stilla, Ross Glasscock and others lost to CJD.

Compliance with Ethical Standards

Conflict of interest There are no conflicts of interest to declare.

References

1. Morales R, Duran-Aniotz C, Diaz-Espinoza R, Camacho MV, Soto C (2012) Protein misfolding cyclic amplification of infectious prions. Nat Protoc 7:1397–1409
2. Lee KS, Caughey B (2007) A simplified recipe for prions. Proc Natl Acad Sci USA 104:9551–9552
3. Wang F, Wang X, Yuan C-G, Ma J (2010) Generating a prion with bacterially expressed recombinant prion protein. Science 327:1132–1135
4. Wang F, Wang X, Ma J (2011) Conversion of bacterially expressed recombinant prion protein. Methods 53:208–213
5. Zhang Z, Zhang Y, Wang F, Wang X, Xu Y, Yang H, Yu G, Yuan C, Ma J (2013) De novo generation of infectious prions with bacterially expressed recombinant prion protein. FASEB J 27:4768–4775
6. Wang F, Zhang Z, Wang X, Li J, Zha L, Yuan CG, Weissmann C, Ma J (2012) Genetic informational RNA is not required for recombinant prion infectivity. J Virol 86:1874–1876
7. Kim JI, Cali I, Surewicz K, Kong Q, Raymond GJ, Atarashi R, Race B, Qing L, Gambetti P, Caughey B, Surewicz WK (2010) Mammalian prions generated from bacterially expressed prion protein in the absence of any mammalian cofactors. J Biol Chem 285:14083–14087
8. Deleault NR, Piro JR, Walsh DJ, Wang F, Ma J, Geoghegan JC, Supattapone S (2012) Isolation of phosphatidylethanolamine as a solitary cofactor for prion formation in the absence of nucleic acids. Proc Natl Acad Sci USA 109:8546–8551
9. Haigh CL, Drew SC (2015) Cavitation during the protein misfolding cyclic amplification (PMCA) method—the trigger for de novo prion generation? Biochem Biophys Res Commun 461:494–500
10. Nash T (1953) The colorimetric estimation of formaldehyde by means of the Hantzsch reaction. Biochem J 55:416–421
11. Belman S (1963) The fluorometric determination of formaldehyde. Anal Chim Acta 29:120–126
12. Li Q, Sritharathikhun P, Motomizu S (2007) Development of novel reagent for Hantzsch reaction for the determination of formaldehyde by spectrophotometry and fluorometry. Anal Sci 23:413–417
13. Wobbrock J, Findlater L, Gergle D, Higgins J (2011) The aligned rank transform for nonparametric factorial analyses using only ANOVA procedures. In: Proceedings of the ACM conference on human factors in computing systems (CHI 2011), Vancouver, British Columbia (May 7–12). New York: ACM Press, pp 143–146. https://depts.washington.edu/aimgroup/proj/art/. https://doi.org/10.1145/1978942.1978963
14. Shiraishi H, Kataoka M, Morita Y, Umemoto J (1993) Interactions of hydroxyl radicals with tris (hydroxymethyl) aminomethane and Good's buffers containing hydroxymethyl or hydroxyethyl residues produce formaldehyde. Free Radic Res Commun 19:315–321
15. McElroy WJ, Waygood SJ (1991) Oxidation of formaldehyde by the hydroxyl radical in aqueous solution. J Chem Soc Faraday Trans 87:1513–1521
16. Neppiras EA (1980) Acoustic cavitation thresholds and cyclic processes. Ultrasonics 18:201–209
17. Santos HM, Lodeiro C, Capelo-Martinez J-L (2009) The power of ultrasound. In: Capelo-Martínez J-L (ed) Ultrasound in chemistry: analytical applications. Wiley-VCH Verlag GmbH & Co. KGaA, Weinheim

18. Barria MA, Gonzalez-Romero D, Soto C (2012) Cyclic amplification of prion protein misfolding. Methods Mol Biol 849:199–212
19. Park J-H, Choi Y-G, Park S-J, Choi H-S, Choi E-K, Kim Y-S (2018) Ultra-efficient amplification of abnormal prion protein by modified protein misfolding cyclic amplification with electric current. Mol Neurobiol 55:1630–1638
20. Alegria AE, Lion Y, Kondo T, Riesz P (1989) Sonolysis of aqueous surfactant solutions, probing the interfacial region of cavitation bubbles by spin trapping. J Phys Chem 93:4908–4913
21. von Sonntag C (2006) Free-radical-induced DNA damage and its repair—a chemical perspective. Springer, Berlin
22. Munter R (2001) Advanced oxidation processes—current status and prospects. Proc Estonian Acad Sci Chem 50:59–80
23. Adewuyi YG (2005) Sonochemistry in environmental remediation. 1. Combinative and hybrid sonophotochemical oxidation processes for the treatment of pollutants in water. Environ Sci Technol 39:3409–3420
24. Adewuyi YG (2005) Sonochemistry in environmental remediation. 2. Heterogeneous sonophotocatalytic oxidation processes for the treatment of pollutants in water. Environ Sci Technol 39:8557–8570
25. Perkowski J, Mayer J, Kos L (2005) Reactions of non-ionic surfactants, Triton X-n type, with OH radicals: a review. Fibres Text East Eur 13:81–85
26. Levine RL (2002) Carbonyl modified proteins in cellular regulation, aging, and disease. Free Radic Biol Med 32:790–796
27. Dalle-Donne I, Rossi R, Giustarini D, Milzani A, Colombo R (2003) Protein carbonyl groups as biomarkers of oxidative stress. Clin Chim Acta 329:23–38
28. Talpaert-Borlè M (1987) Formation, detection and repair of AP sites. Mutat Res 181:45–56
29. Zhang X, Barraza KM, Beauchamp JL (2018) Cholesterol provides nonsacrificial protection of membrane lipids from chemical damage at air–water interface. Proc Natl Acad Sci USA 115:3255–3260
30. Höbel B, von Sonntag C (1998) OH-radical induced degradation of ethylenediaminetetraacetic acid (EDTA) in aqueous solution: a pulse radiolysis study. J Chem Soc Perkin Trans 2:509–514
31. McGhee JD, von Hippel PH (1975) Formaldehyde as a probe of DNA structure. I. Reaction with exocyclic amino groups of DNA bases. Biochemistry 14:1281–1296
32. McGhee JD, von Hippel PH (1975) Formaldehyde as a probe of DNA structure. II. Reaction with endocyclic imino groups of DNA bases. Biochemistry 14:1297–1303
33. Hemminki K, Suni R (1984) Sites of reaction of glutaraldehyde and acetaldehyde with nucleosides. Arch Toxicol 55:186–190
34. McMurray JE (2012) Organic chemistry, 8th edn. Brooks/Cole, Belmont
35. Feldman MY (1973) Reactions of nucleic acids and nucleoproteins with formaldehyde. Prog Nucleic Acids Res Mol Biol 13:1–49
36. Chaw YFM, Crane LE, Lange P, Shapiro R (1980) Isolation and identification of cross-links from formaldehyde-treated nucleic acids. Biochemistry 19:5525–5531
37. Kuykendall JR, Bogdanffy MS (1994) Formation and stability of acetaldehyde-induced crosslinks between poly-lysine and polydeoxyguanosine. Mutat Res 311:49–56
38. Shaham J, Bomstein Y, Meltzer A, Kaufman Z, Palma E, Ribak J (1996) DNA-protein crosslinks, a biomarker of exposure to formaldehyde—in vitro and in vivo studies. Carcinogenesis 17:121–125
39. Han Y, Shchukin D, Schneider J, Möhwald H (2014) Fluorescence indicative pH drop in sonication. Colloids Surf A Physicochem Eng Asp 445:30–33
40. Mark G, Schuchmann H-P, von Sonntag C (2000) Formation of peroxynitrite by sonication of aerated water. J Am Chem Soc 122:3781–3782
41. Swietnicki W, Petersen R, Gambetti P, Surewicz WK (1997) pH-dependent stability and conformation of the recombinant human prion protein PrP(90–231). J Biol Chem 272:27517–27520
42. Arnold JE, Tipler C, Laszlo L, Hope J, Landon M, Mayer RJ (1995) The abnormal isoform of the prion protein accumulates in late-endosome-like organelles in scrapie-infected mouse brain. J Pathol 176:403–411
43. Borchelt DR, Taraboulos A, Prusiner SB (1992) Evidence for synthesis of scrapie prion proteins in the endocytic pathway. J Biol Chem 267:16188–16199
44. Tretyakova NY, Groehler A IV, Ji S (2015) DNA-protein cross-links: formation, structural identities, and biological outcomes. Acc Chem Res 48:1631–1644
45. Pacher P, Beckman JS, Liaudet L (2007) Nitric oxide and peroxynitrite in health and disease. Physiol Rev 87:315–424
46. Klunk WE, Pettegrew JW (1990) Alzheimer's beta-amyloid protein is covalently modified when dissolved in formic acid. J Neurochem 54:2050–2056
47. Shishodia S, Zhang D, El-Sagheer AH, Brown T, Claridge TDW, Schofield CJ, Hopkinson RJ (2018) NMR analyses on N-hydroxymethylated nucleobases—implications for formaldehyde toxicity and nucleic acid demethylases. Org Biomol Chem 16:4021–4032
48. Edrissi B, Taghizadeh K, Dedon PC (2013) Quantitative analysis of histone modifications: formaldehyde is a source of pathological N6-formyllysine that is refractory to histone deacetylases. PLoS Genet 9:e1003328
49. Zhang L, Freeman LE, Nakamura J, Hecht SS, Vandenberg JJ, Smith MT, Sonawane BR (2010) Formaldehyde and leukemia: epidemiology, potential mechanisms, and implications for risk assessment. Environ Mol Mutagen 51:181–191
50. Su T, Monte WC, Hu X, He Y, He R (2016) Formaldehyde as a trigger for protein aggregation and potential target for mitigation of age-related, progressive cognitive impairment. Curr Top Med Chem 16:472–484
51. Green AJE (2019) RT-QuIC: a new test for sporadic CJD. Pract Neurol 19:49–55
52. Raymond GJ, Race B, Orrú CD, Raymond LD, Bongianni M, Fiorini M, Groveman BR, Ferrari S, Sacchetto L, Hughson AG, Monaco S, Pocchiari M, Zanusso G, Caughey B (2020) Transmission of CJD from nasal brushings but not spinal fluid or RT-QuIC product. Ann Clin Transl Neurol 7:932–944
53. Koda S, Kimura T, Kondo T, Mitome H (2003) A standard method to calibrate sonochemical efficiency of an individual reaction system. Ultrason Sonochem 10:149–156
54. Ashokkumar M, Niblett T, Tantiongco L, Grieser F (2003) Sonochemical degradation of sodium dodecylbenzene sulfonate in aqueous solutions. Aust J Chem 56:1045–1049
55. Merouani S, Hamdaoui O, Saoudi F, Chiha M (2010) Influence of experimental parameters on sonochemistry dosimetries: KI oxidation, Fricke reaction and H_2O_2 production. J Hazard Mater 178:1007–1014
56. Yamaguchi K, Matsumoto T, Kuwata K (2012) Proper calibration of ultrasonic power enabled the quantitative analysis of the ultrasonication-induced amyloid formation process. Protein Sci 21:38–49